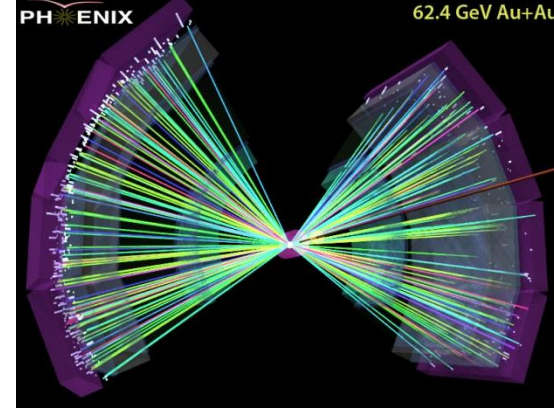
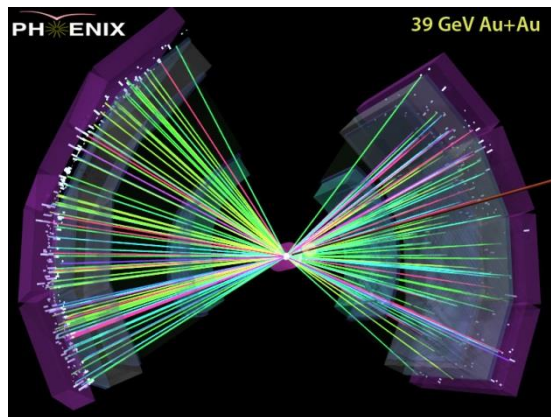
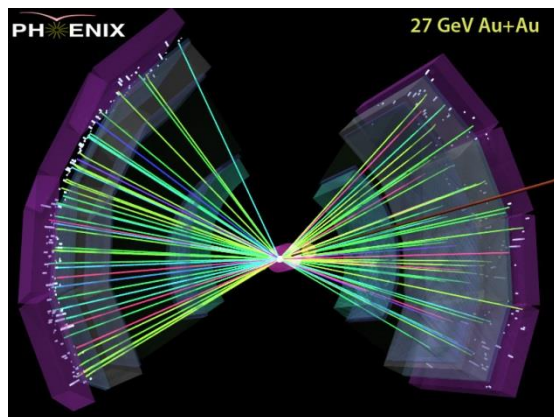
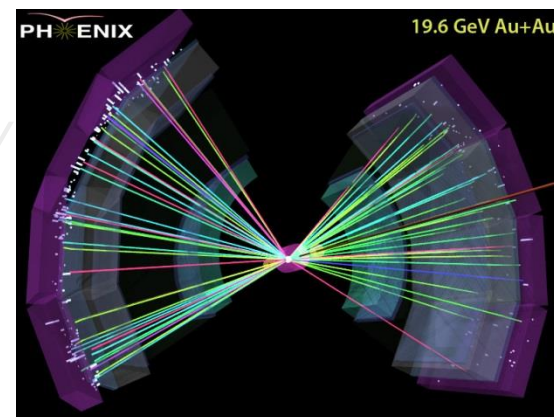
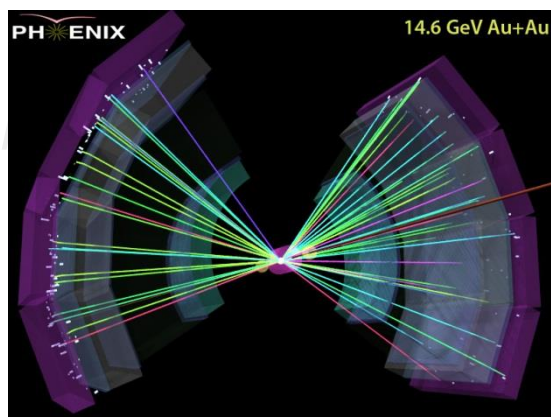
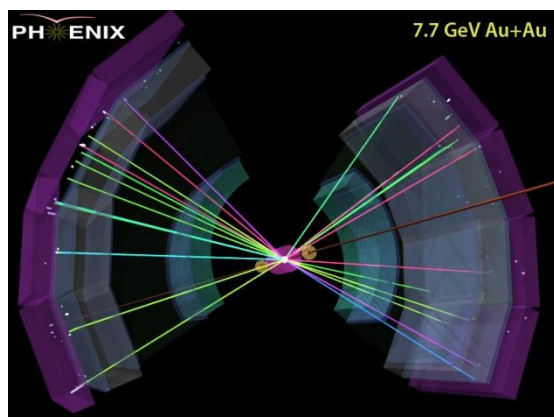


Global Observable Measurements from the Beam Energy Scan in PHENIX



Jeffery T. Mitchell for the PHENIX Collaboration



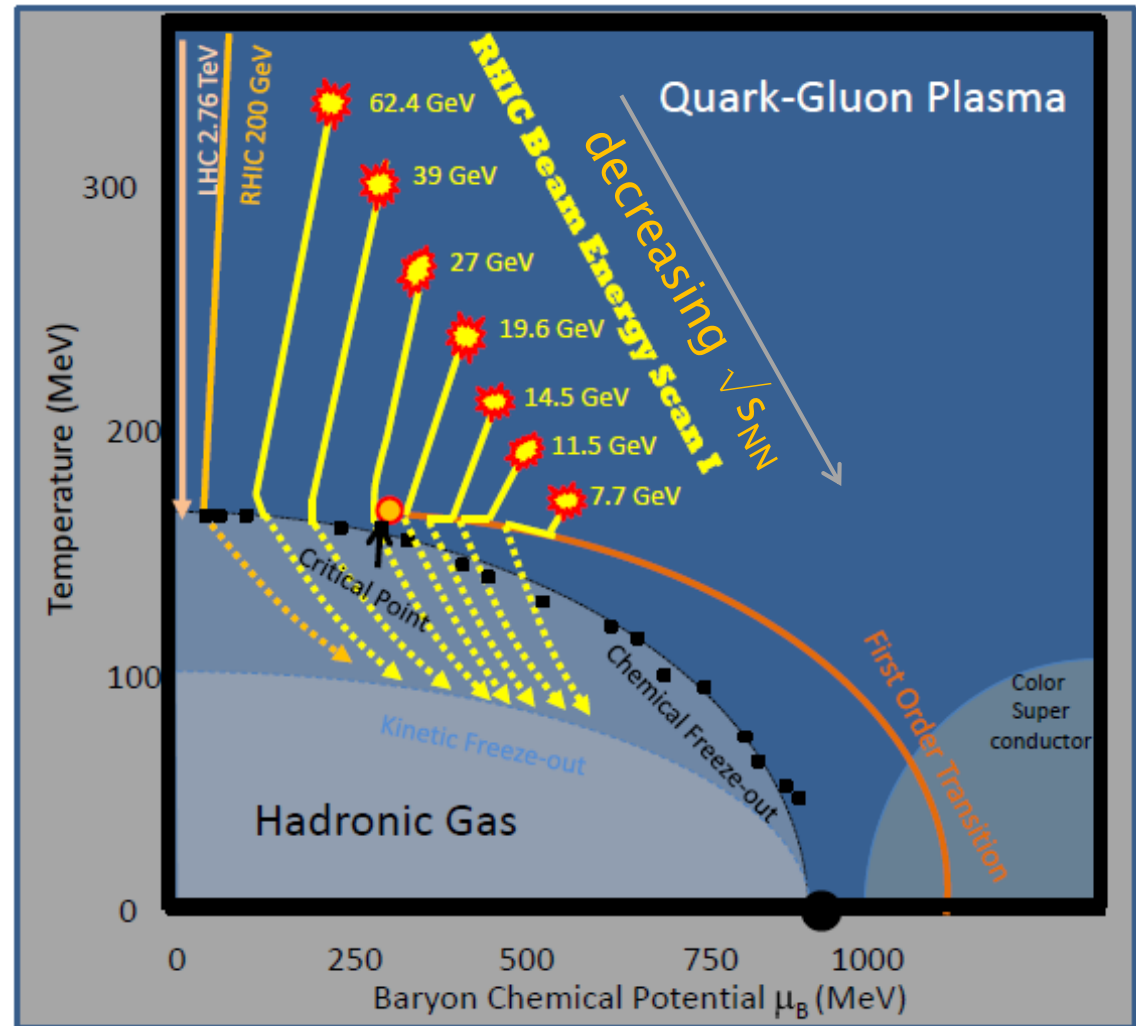
The RHIC Beam Energy Scan Program: Probing the Nuclear Matter Phase Diagram

By systematically varying the RHIC beam energy, heavy ion collisions will be able to probe different regions of the QCD phase diagram.

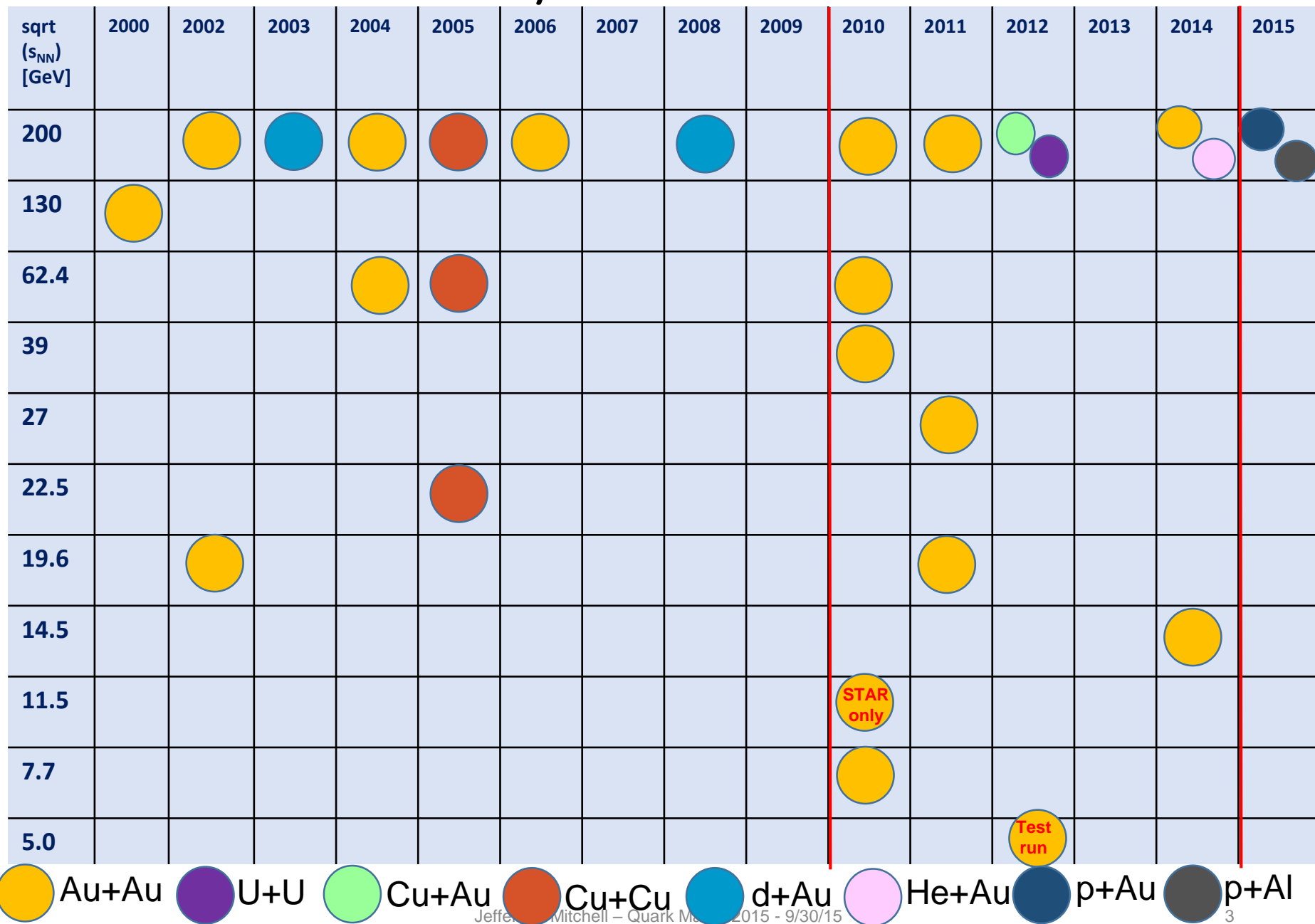
PHENIX is searching for signatures of the onset of deconfinement and searching for signatures of the critical point.

Outline:

- Collision Energy Dependence
- Participant Nucleon Scaling
- System Size Dependence
- Participant Quark Scaling
- Flow
- Summary



The PHENIX Heavy Ion Datasets: An Overview



PHENIX Transverse Energy and Charged Particle Multiplicity Datasets

$\sqrt{s_{NN}}$ (GeV)	System	Year	N_{events}
200	Au+Au	2002	270 k
200	Au+Au	2004	133 M
130	Au+Au	2000	160 k
62.4	Au+Au	2004	20 M
62.4	Au+Au	2010	12 M
39	Au+Au	2010	132 M
27	Au+Au	2011	24.5 M
19.6	Au+Au	2011	6.3 M
14.5	Au+Au	2014	6.8 M
7.7	Au+Au	2010	803 k
200	Cu+Cu	2005	558 M
62.4	Cu+Cu	2005	175 M
200	Cu+Au	2012	2.6 B
193	U+U	2012	317 M
200	$^3\text{He}+\text{Au}$	2014	1.6 B
200	$d+\text{Au}$	2008	1.4 B
200	$p+p$	2003	14.6 M

A comprehensive survey of E_T and N_{ch} production has been recently submitted to the arXiv:
arXiv:1509.06727

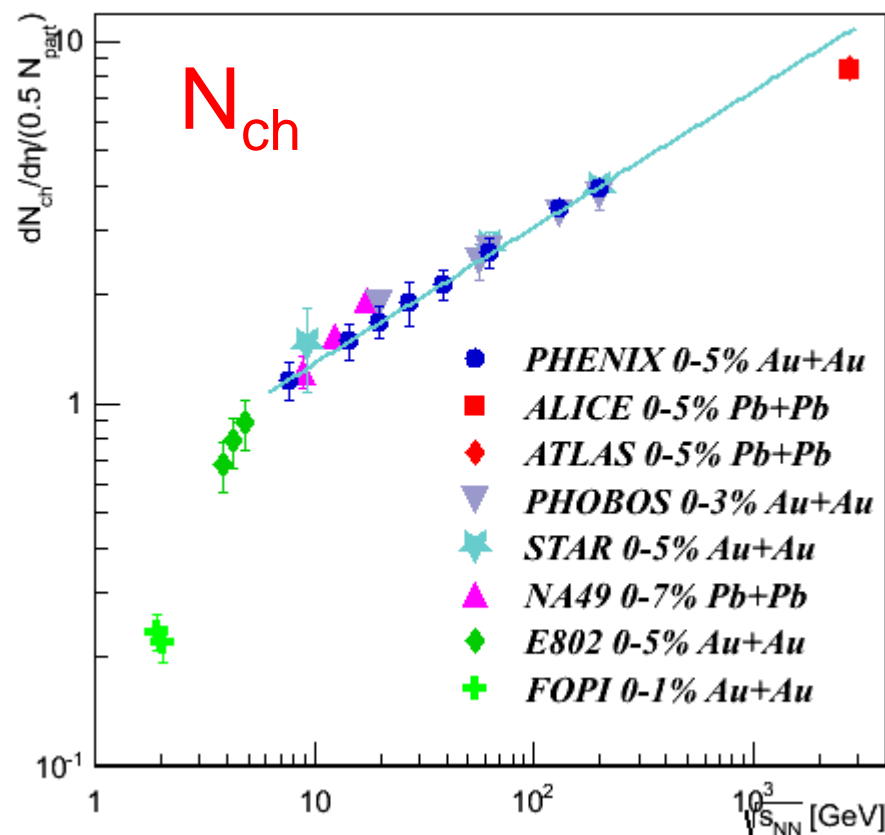
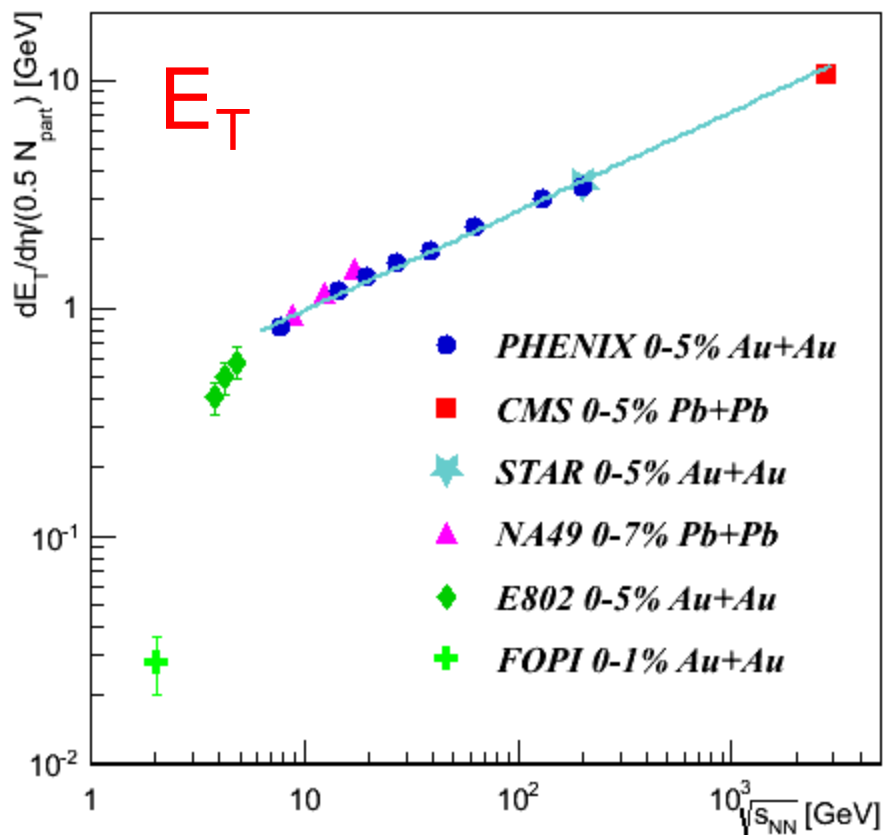
We can investigate the collision energy dependence and the system size dependence of E_T and N_{ch} production with 15 different collision systems.

Transverse Energy and Charged Particle Production Excitation Function

Mid-rapidity

arXiv:1509.06727

Central collisions

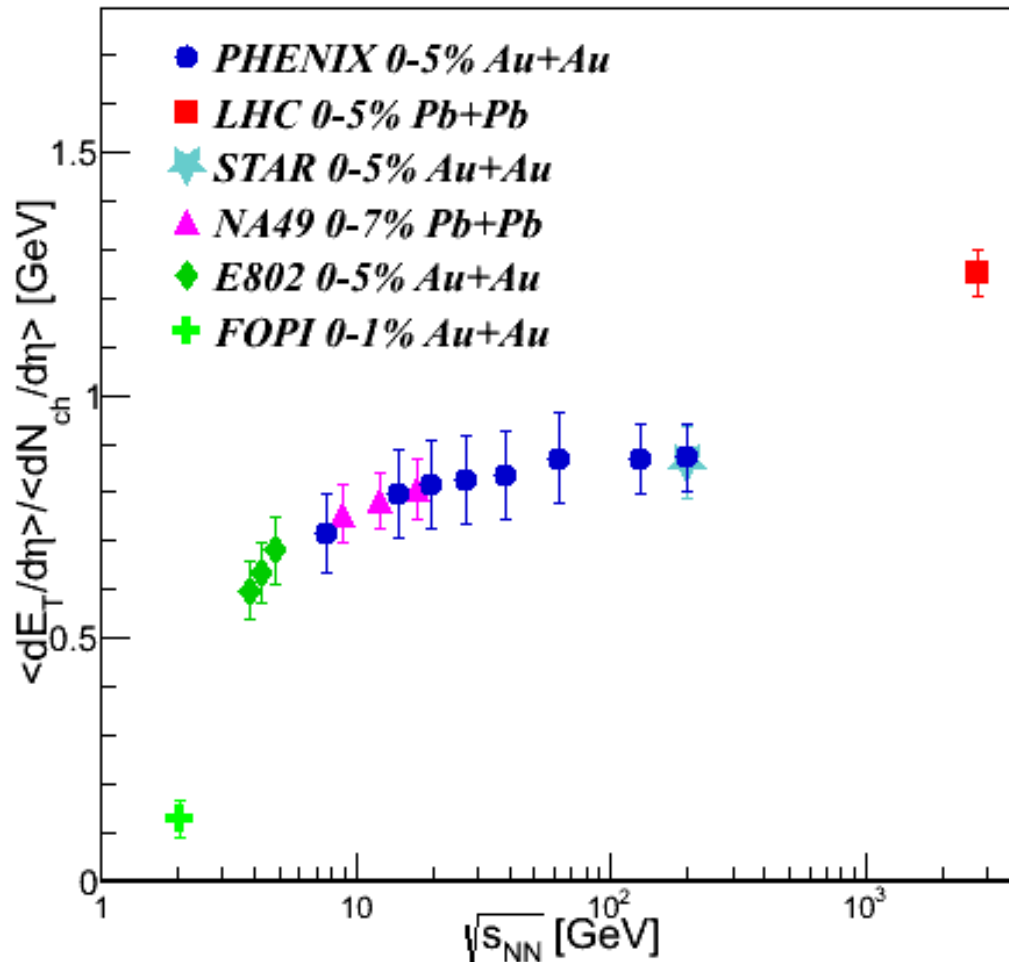


From 7.7-200 GeV, both transverse energy and charged particle multiplicity follow a power law behavior.

Transverse Energy Per Charged Particle: Excitation Function

Mid-rapidity

Central collisions



There is very little change in the transverse energy per charged particle from 7.7 GeV to 200 GeV.

There is an increase at LHC energies.

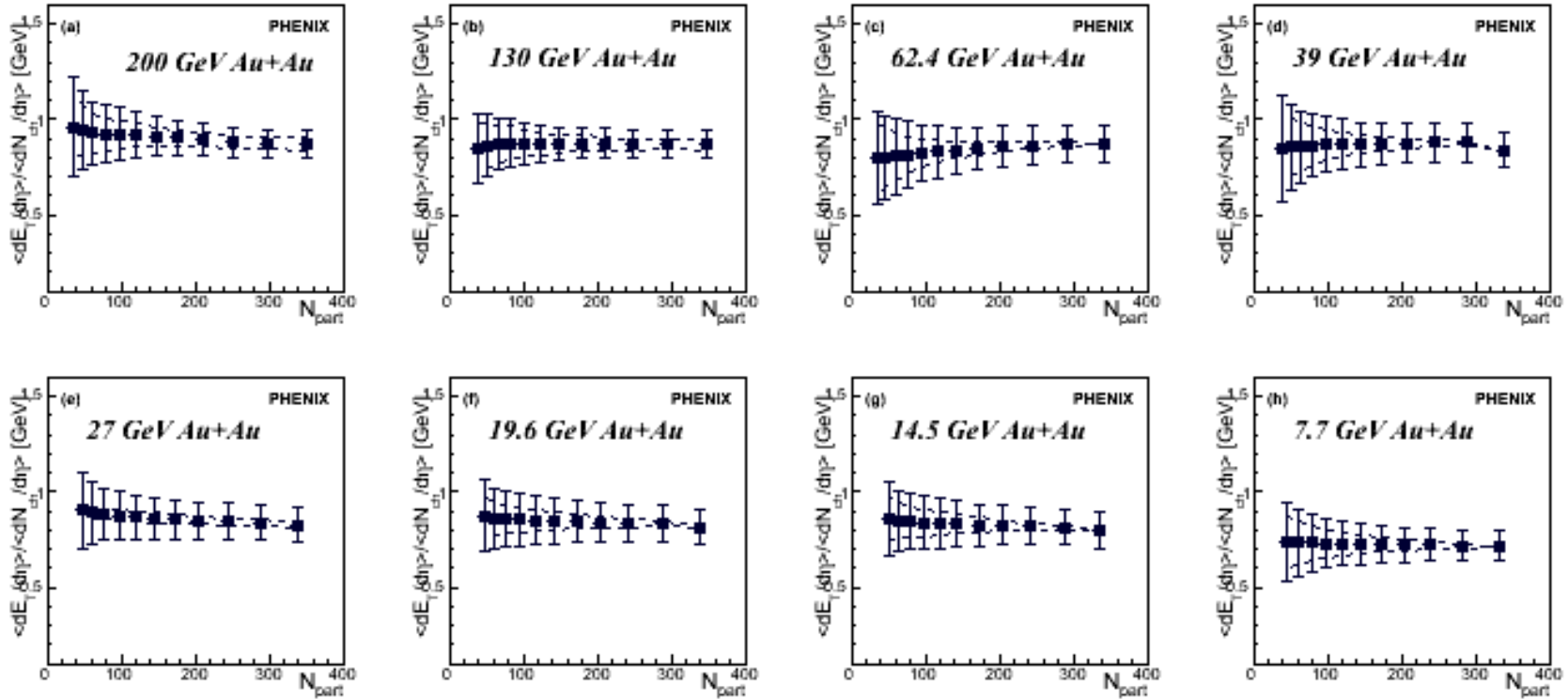
The LHC point uses CMS E_T (PRL 109, 152303 (2012)) and the average of ALICE (PRL 106, 032301 (2011)) and ATLAS (Phys. Lett. B710, 363 (2012)) N_{ch} data.

arXiv:1509.06727

Transverse Energy Per Charged Particle: Centrality Dependence

arXiv:1509.06727

Mid-rapidity

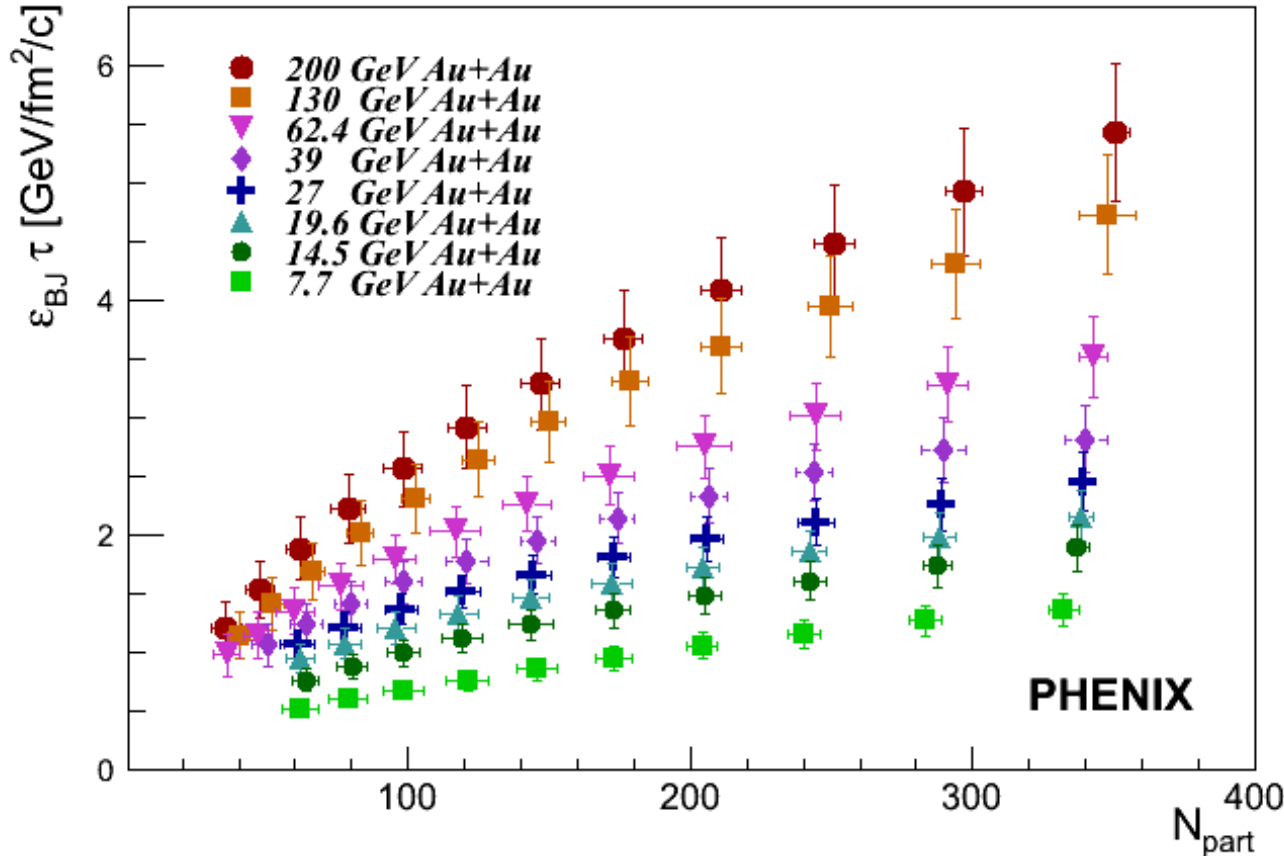


The error bars represent statistical + systematic uncertainties. The dashed error bands represent the trigger efficiency uncertainty within which the points can be tilted.

The $\langle dE_T/d\eta \rangle / \langle dN_{ch}/d\eta \rangle$ ratio is independent of centrality for all collision energies.

Bjorken Energy Density: Centrality Dependence

Mid-rapidity



arXiv:1509.06727

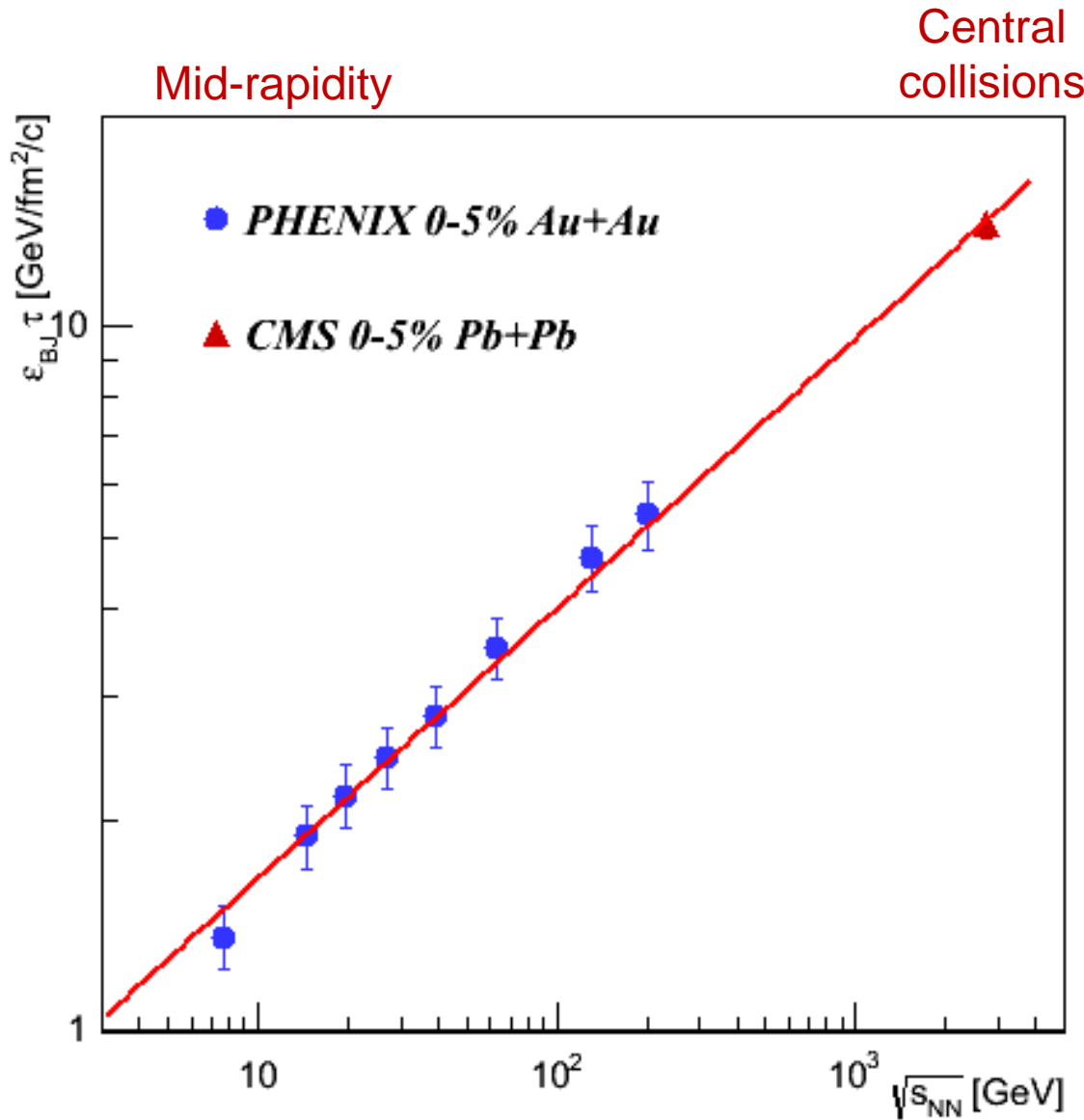
$$\epsilon_{Bj} = \frac{1}{A_{\perp} \tau} \frac{dE_T}{dy}$$

A_{\perp} is estimated using a Glauber Monte Carlo:

$$A_{\perp} \sim \sigma_x \sigma_y$$

ϵ_{Bj} for central collisions increases by a factor of 3.8 when going from 7.7 to 200 GeV.

Bjorken Energy Density Excitation Function



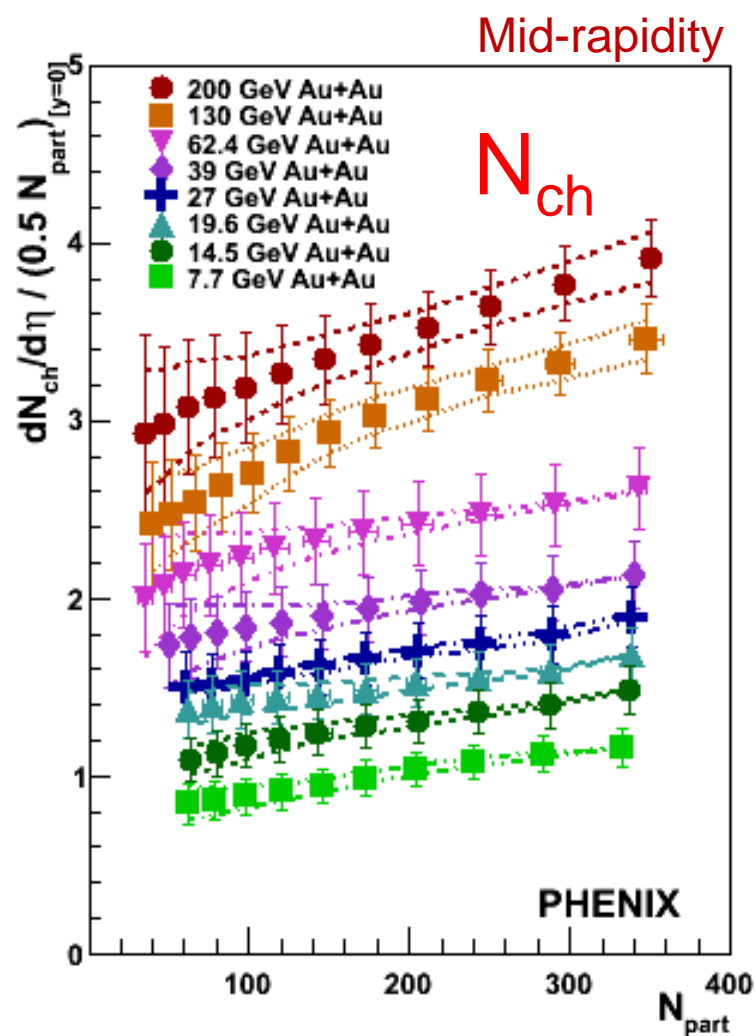
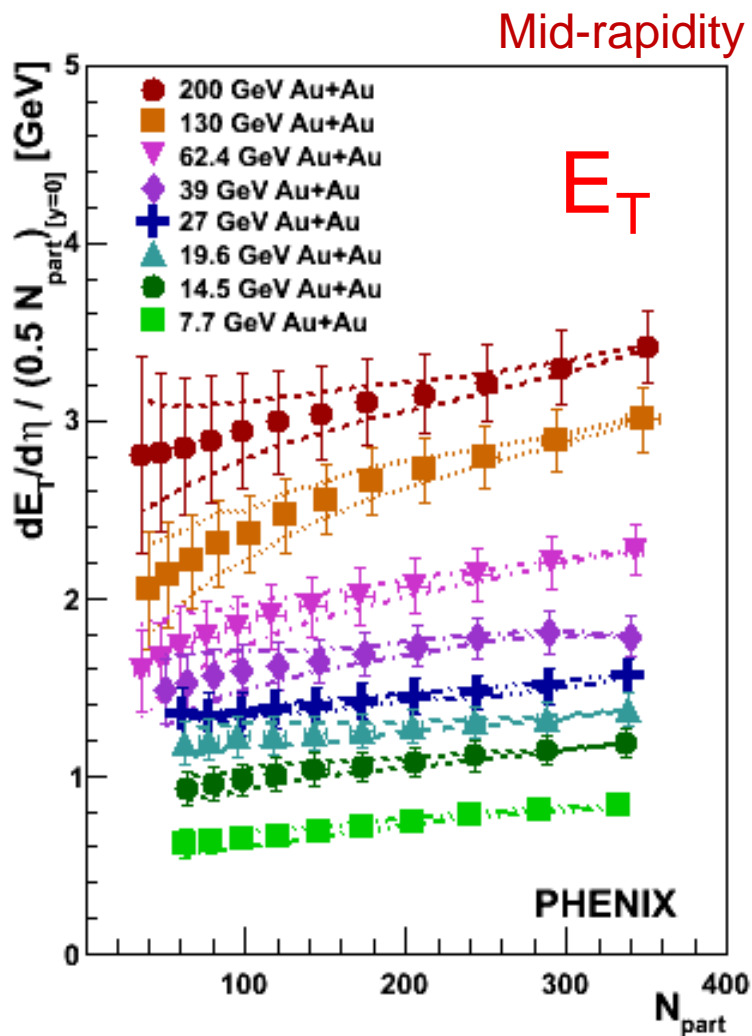
$$\epsilon_{Bj} = \frac{1}{A_{\perp} \tau} \frac{dE_T}{dy}$$

Over this collision energy range, the Bjorken energy density follows a power law behavior. The line is a power law fit to all of the points shown. The exponent is 0.38 ± 0.01 .

The CMS data point is from Phys. Rev. Lett. 109, 152303 (2012).

arXiv:1509.06727

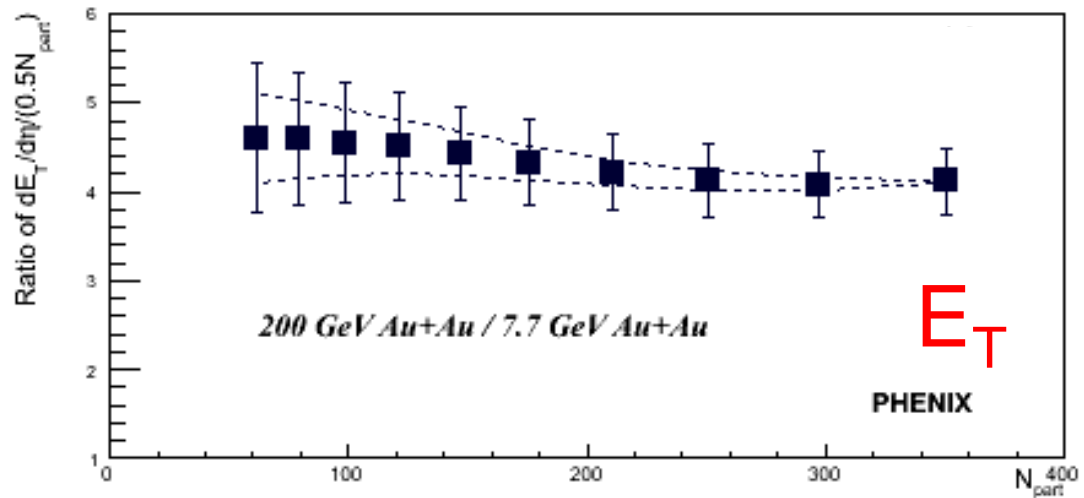
Participant Nucleon Scaling: Au+Au Beam Energy Scan



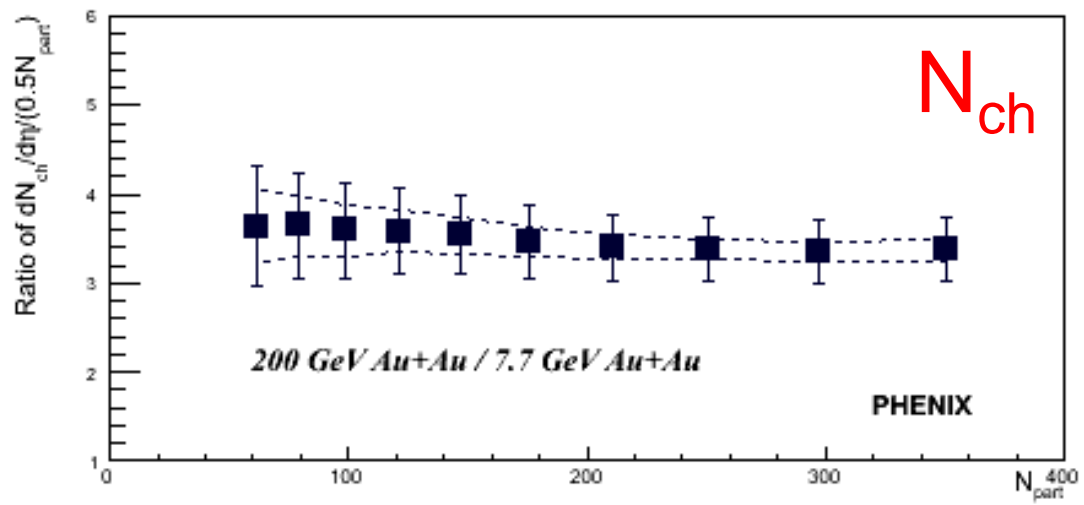
*Phys. Rev. C*71 (2005) 034908.
*Phys. Rev. C*89 (2014) 044905.
arXiv:1509.06727

The data increase with collision energy and with N_{part} for all collision energies.

Participant Nucleon Scaling: 200 vs. 7.7 GeV Au+Au



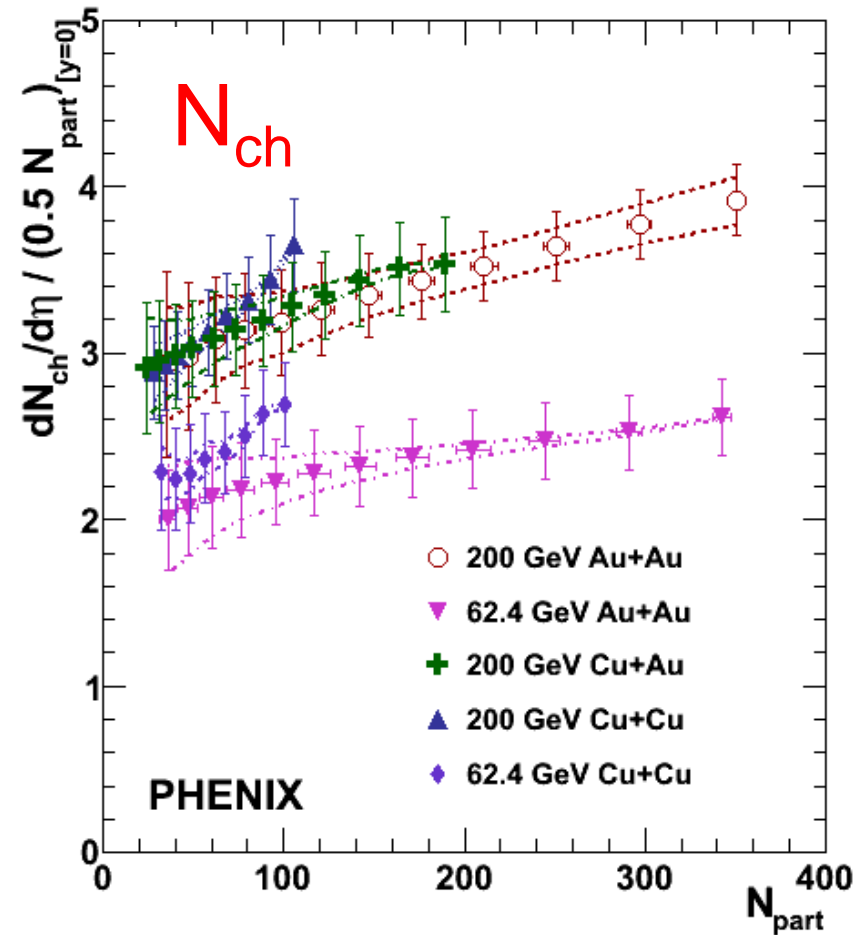
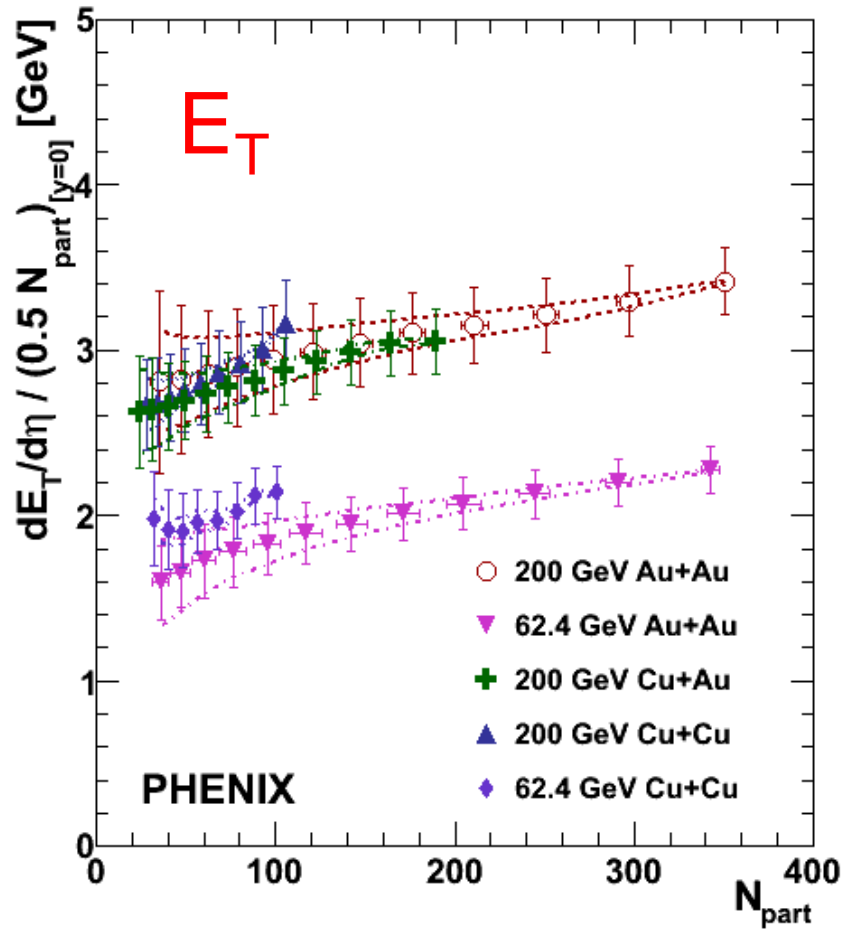
The shapes of the distributions as a function of N_{part} do not change significantly from 200 down to 7.7 GeV.



arXiv:1509.06727

Participant Nucleon Scaling for smaller systems

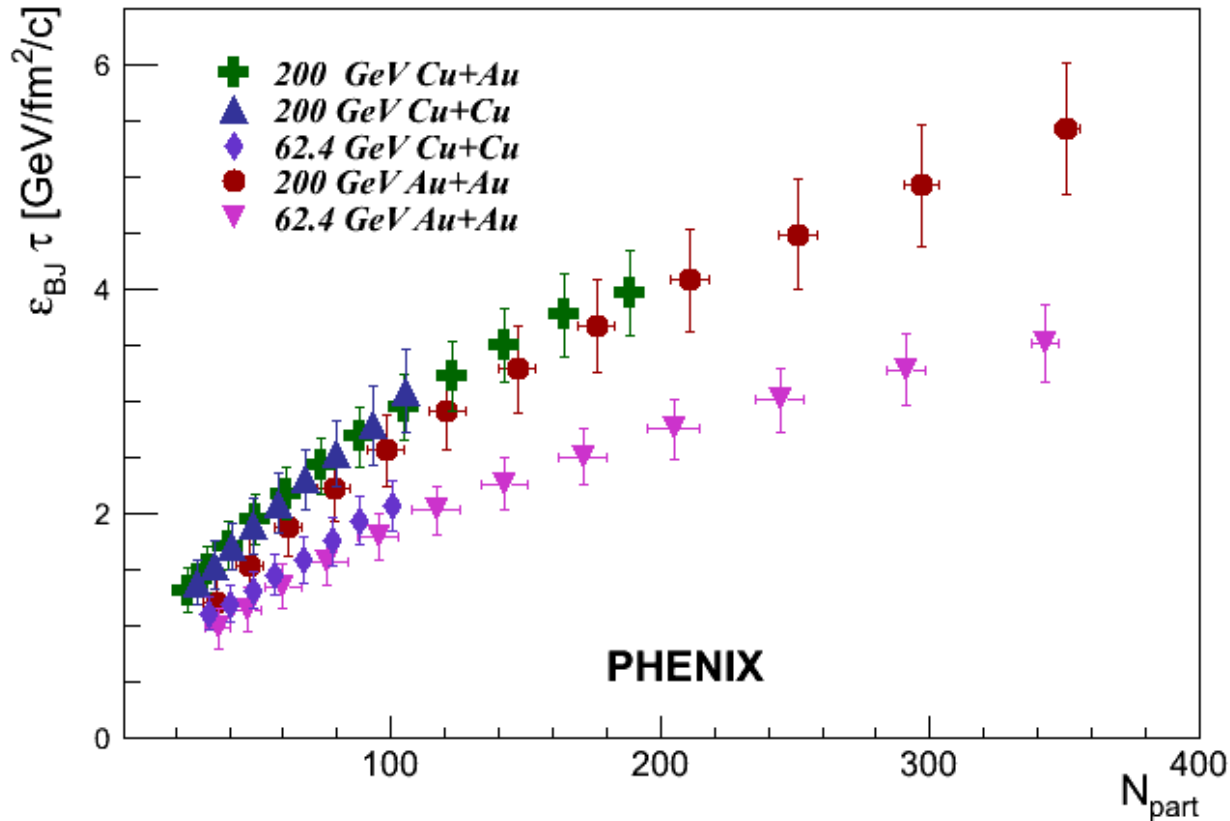
arXiv:1509.06727



The distributions as a function of N_{part} do not change significantly between Au+Au, Cu+Au, and Cu+Cu systems at the same collision energy. For a given collision energy (200 or 62.4 GeV), the data are independent of system size.

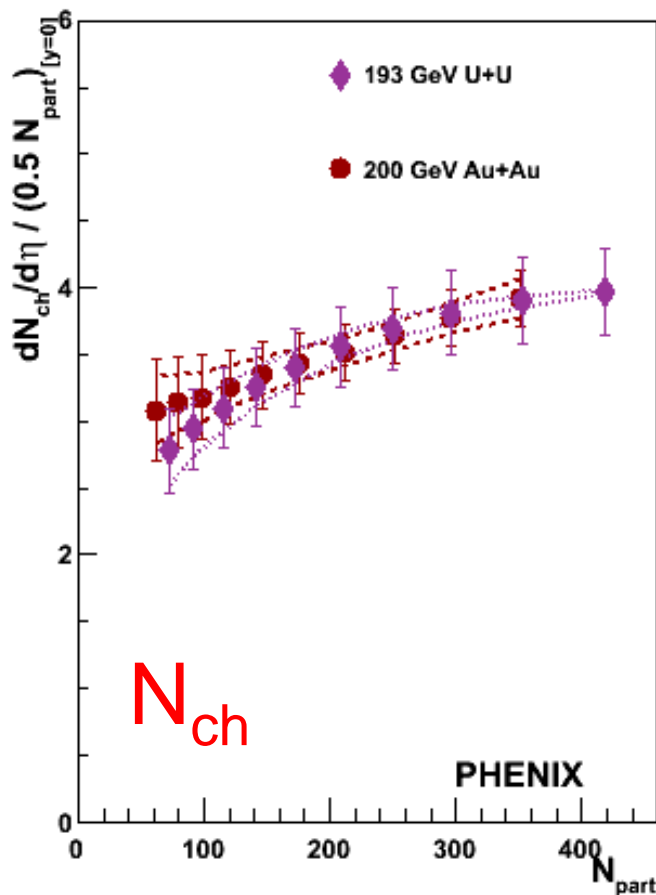
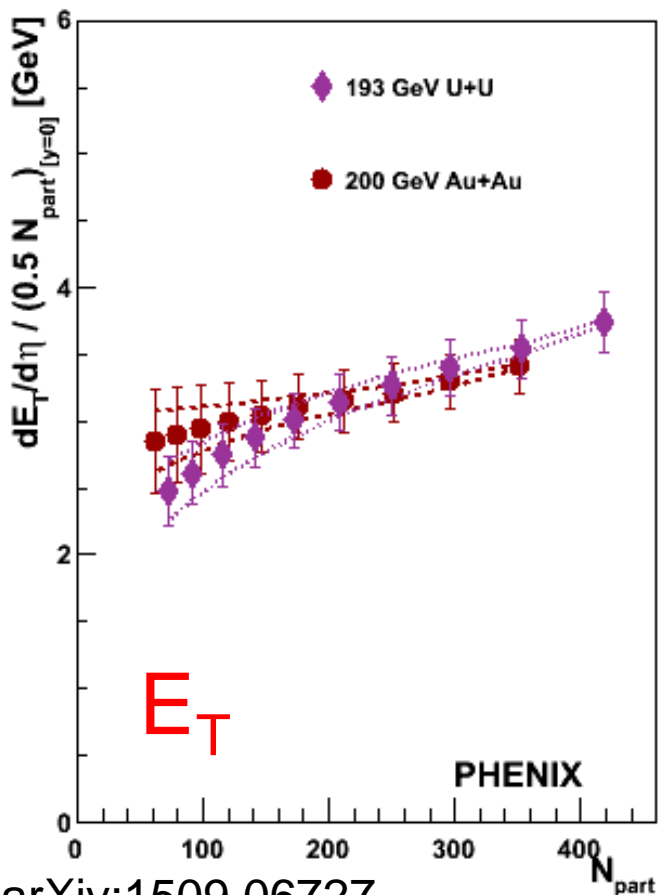
Participant Nucleon Scaling for smaller systems: Bjorken Energy Density

arXiv:1509.06727



The ϵ_{bj} calculation takes the system geometry into account. The distributions as a function of N_{part} do not change significantly between Au+Au, Cu+Au, and Cu+Cu systems at the same collision energy. For a given collision energy (200 or 62.4 GeV), the data are independent of system size.

Participant Nucleon Scaling for U+U



The distributions as a function of N_{part} also do not change significantly between Au+Au and U+U systems.

arXiv:1509.06727

Estimates of N_{part} use a Glauber model with a deformed Woods-Saxon distribution:

$$\rho(r) = \rho_0 / (1 + e^{(r-R')/a}) \quad \text{with} \quad R' = R[1 + \beta_2 Y_2^0(\theta) + \beta_4 Y_4^0(\theta)].$$

Here, $R=6.81$ fm, $a = 0.6$ fm, $\beta_2 = 0.28$, and $\beta_4 = 0.093$.

Estimating the number of constituent quark participants, N_{qp}

$\sqrt{s_{NN}}$ [GeV]	$\sigma_{inelastic}$ [mb]	σ_{qq} [mb]
2760	64.0	18.4
200	42.3	8.17
130	39.6	7.54
62.4	36.0	6.56
39	34.3	6.15
27	33.2	5.86
19.6	32.5	5.70
14.5	32.0	5.58
7.7	31.2	5.35

The number of quark participants is estimated using a modified Glauber model.

Nucleons are replaced by 3 constituent quarks with the center of mass preserved.

The radial distribution is adjusted to reproduce the proton form factor:

$$\rho^{proton}(r) = \rho_0^{proton} \times \exp(-ar)$$

Interactions occur if the following condition is met:

$$d < \sqrt{\frac{\sigma_{qq}^{inel}}{\pi}}$$

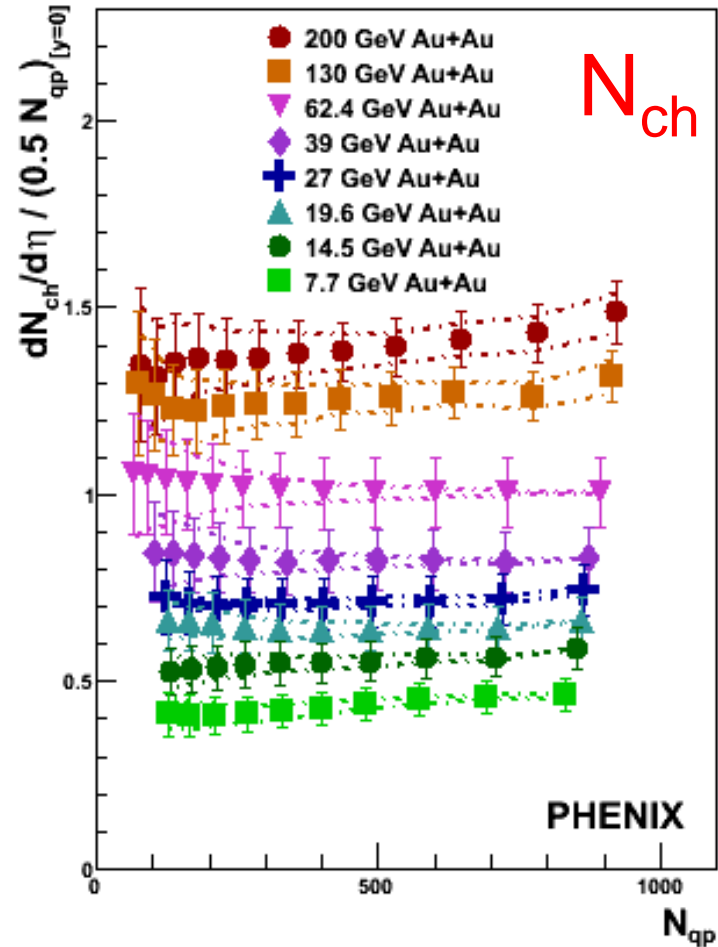
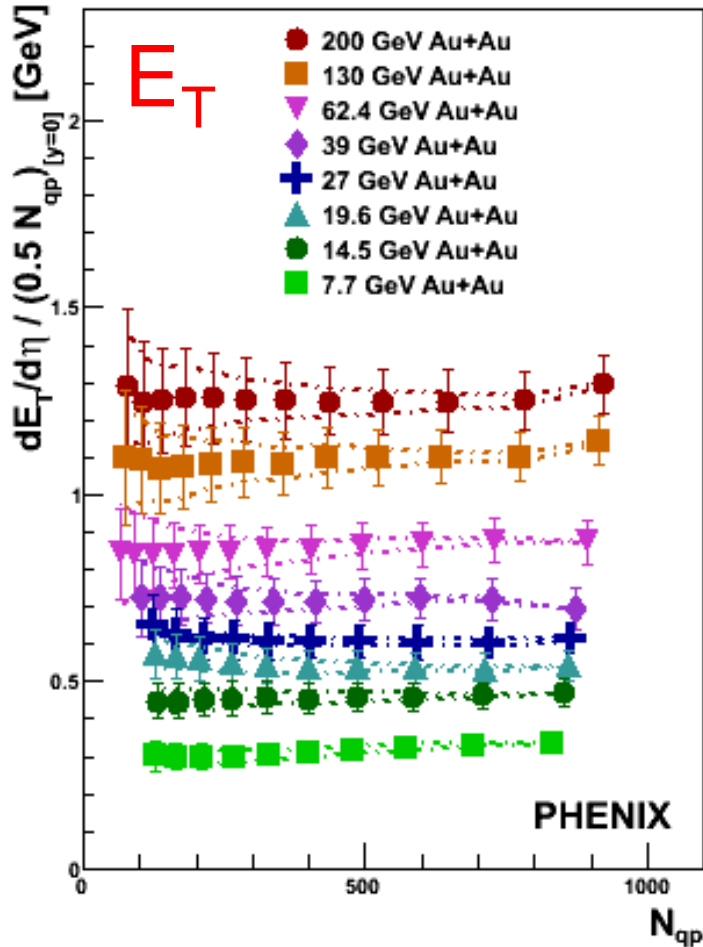
The q-q inelastic cross section is estimated by matching the n-n inelastic cross section in p+p collisions.

N_{qp} as a function of centrality is then estimated using the procedure described in M.L. Miller et al., Ann. Rev. Nucl. Part. Sci. 57, 205 (2007).

Previous studies of quark participants can be found in S. Eremin and S. Voloshin, PRC 67, 064905 (2003) and R. Nouicer, EPJ C49, 281 (2007). Thanks to A. Bzdak for useful discussions.

Participant Quark Scaling: Au+Au Beam Energy Scan

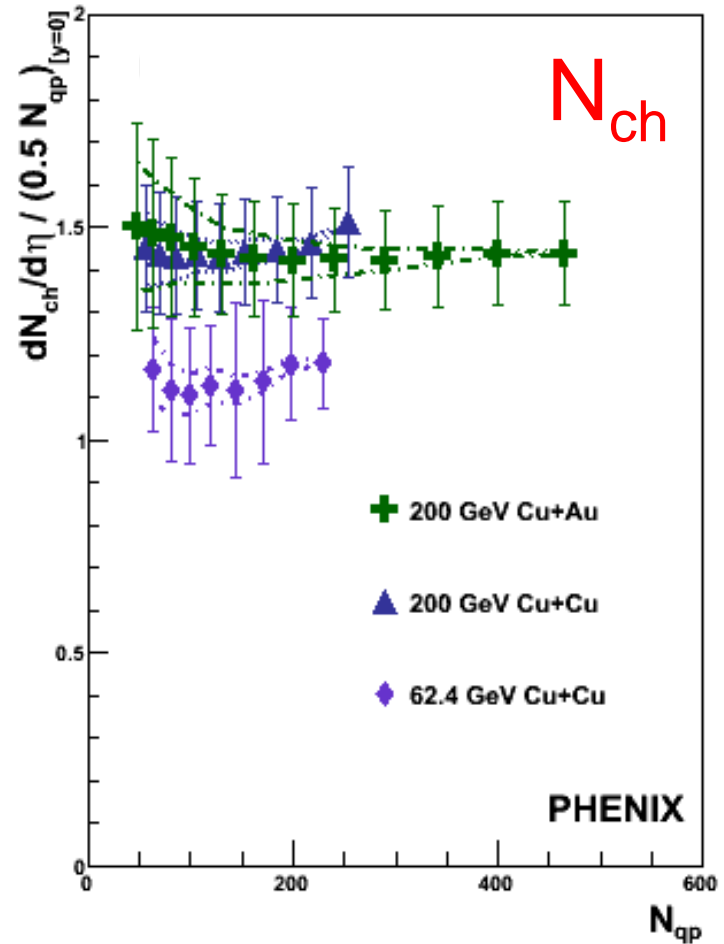
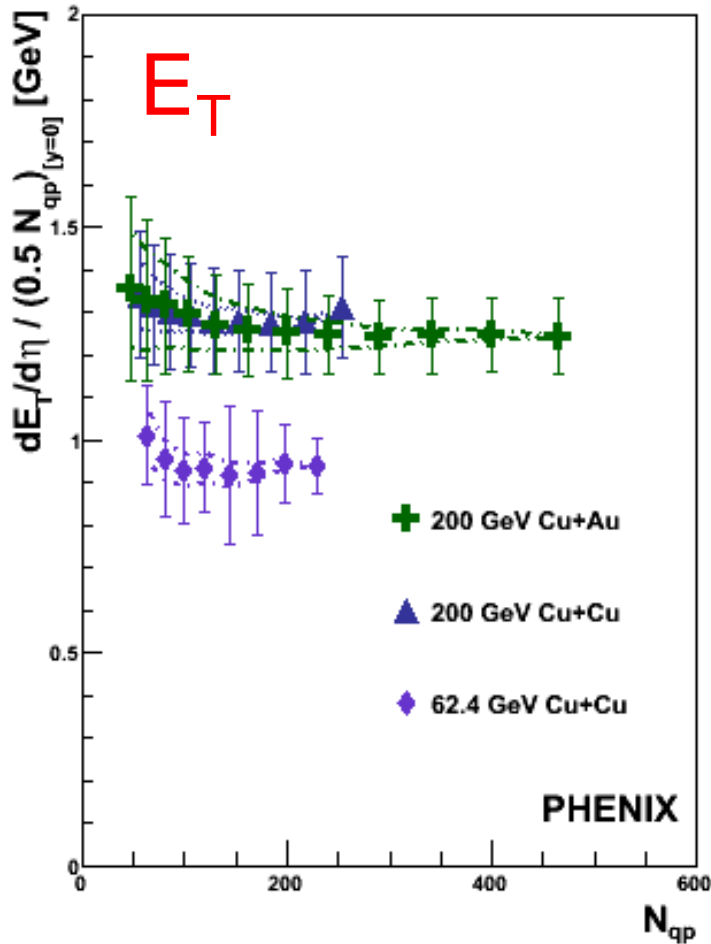
arXiv:1509.06727



Participant quark scaling describes the data better than participant nucleon scaling.

Participant Quark Scaling: Smaller Systems

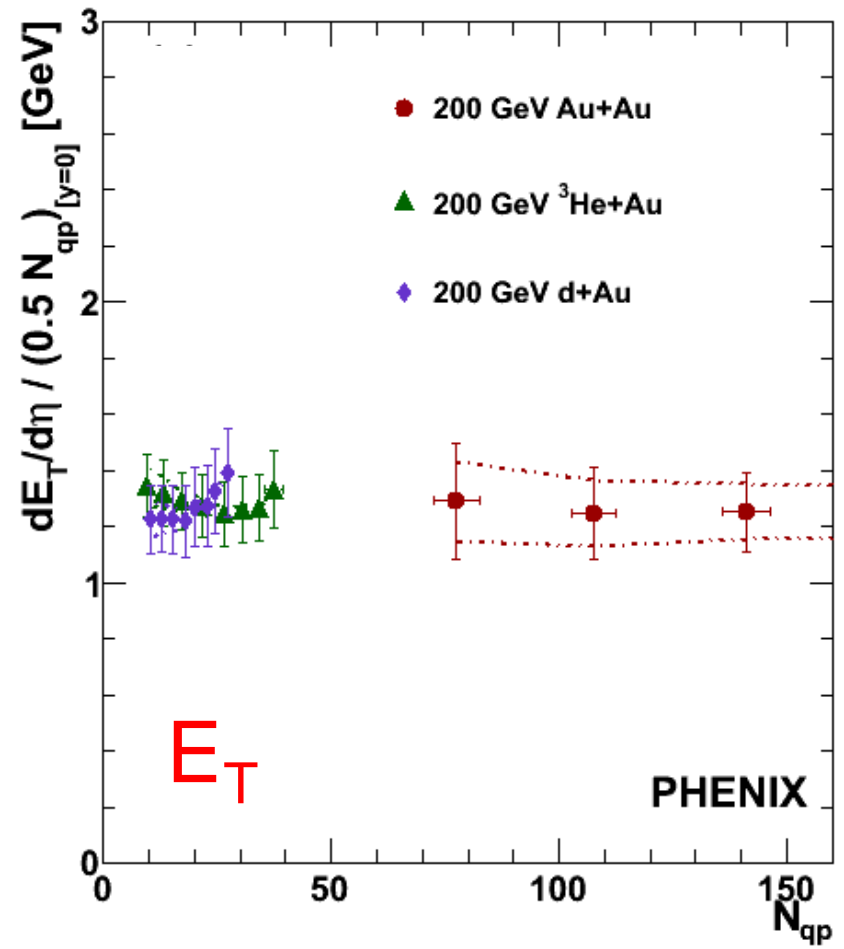
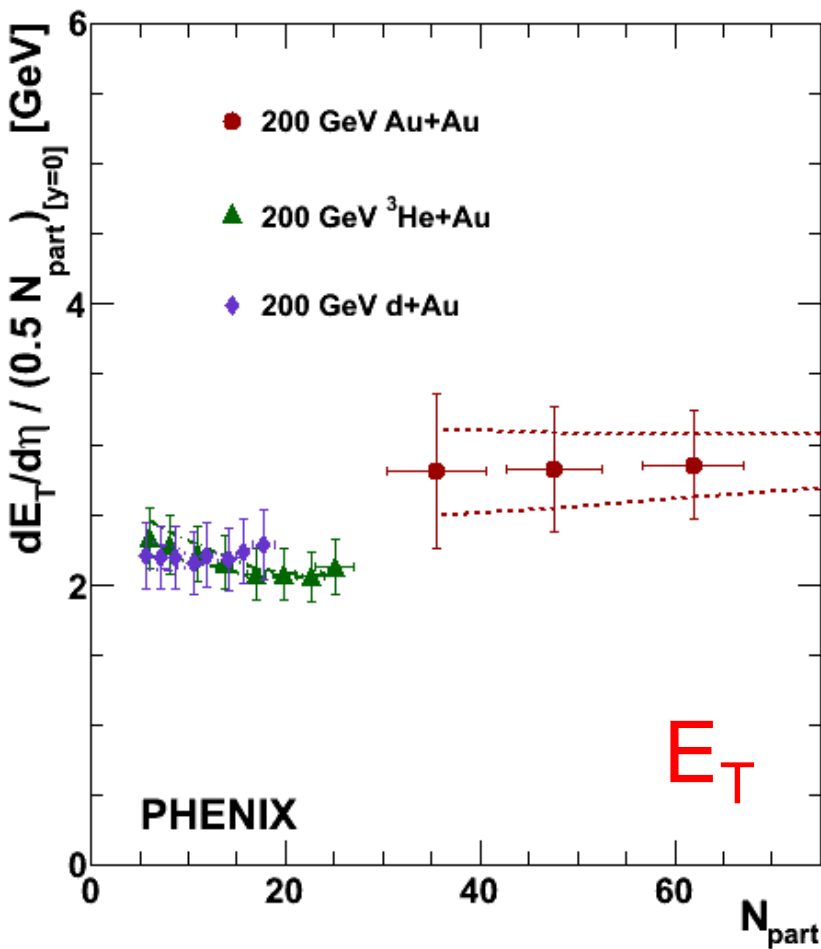
arXiv:1509.06727



Participant quark scaling describes the data better than participant nucleon scaling in the smaller systems, too.

N_{part} vs. N_{qp} scaling for very small systems

arXiv:1509.06727



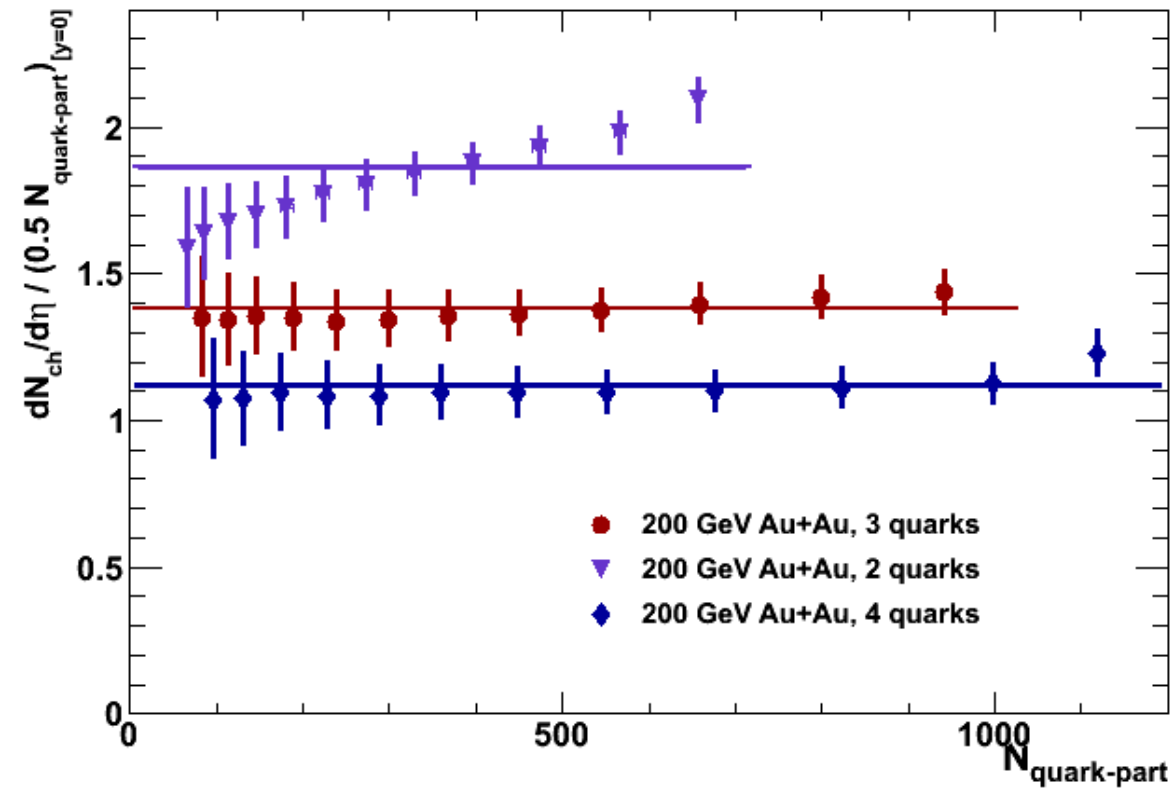
Over the small N_{part} (N_{qp}) range in the small systems, there is no significant distinction between N_{part} or N_{qp} scaling.

Observations

- Bjorken energy density follows a power law behavior from 7.7 GeV to 2.76 TeV.
- The multiplicity and transverse energy data are better described by participant quark scaling than by participant nucleon scaling from 7.7 to 200 GeV.
- Transverse energy and charged particle production is independent of the size of the system at a given collision energy for 62.4 and 200 GeV.
- The ratio of transverse energy to the number of charged particles is independent of centrality from 7.7 to 200 GeV.

Auxiliary Slides

Participant Quark Scaling: Varying the degrees of freedom

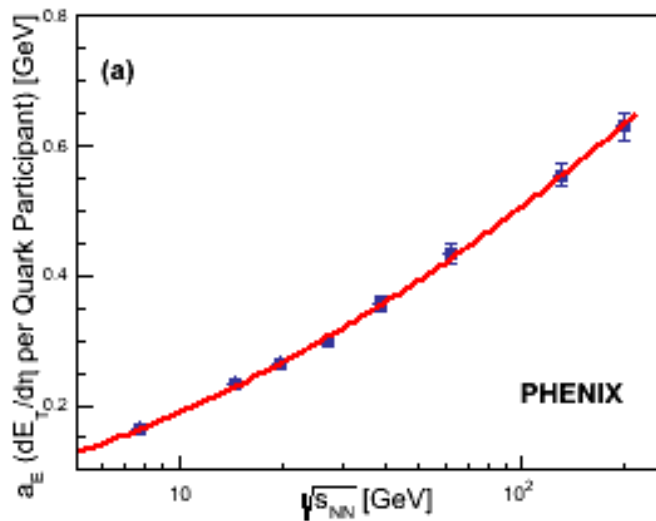


Calculated N_{qp} by distributing 2, 3, and 4 quarks in the modified Glauber model.

For each case, the quark-quark inelastic cross section was adjusted to reproduce the nucleon-nucleon cross section.

The scaling breaks down for the 2 quark case. However the 4 quark case scales well with the exception of the most central point.

$dN/d\eta$ and $dE_T/d\eta$ per Quark Participant



Each point is obtained by fitting $dE_T/d\eta$ or $dN_{ch}/d\eta$ vs. N_{qp} to a straight line. The slope of the fit is plotted.

The slopes increase as the collision energy increases.

The red line is a 2nd-order polynomial fit to all of the data points.

